Atmos. Chem. Phys., 15, 7571–7583, 2015
www.atmos-chem-phys.net/15/7571/2015/
doi:10.5194/acp-15-7571-2015

Atmospheric Chemistry and Physics
Open Access

Reassessing the ratio of glyoxal to formaldehyde as an indicator of hydrocarbon precursor speciation

J. Kaiser[1], G. M. Wolfe[2,3], K. E. Min[4,5,a], S. S. Brown[5,6], C. C. Miller[7], D. J. Jacob[7,8], J. A. deGouw[4,5], M. Graus[4,5], T. F. Hanisco[3], J. Holloway[4,5], J. Peischl[4,5], I. B. Pollack[4,5], T. B. Ryerson[5], C. Warneke[4,5], R. A. Washenfelder[4,5], and F. N. Keutsch[1,b]

[1]Department of Chemistry, University of Wisconsin–Madison, Madison, Wisconsin, USA
[2]Joint Center for Earth Systems Technology, University of Maryland Baltimore County, Baltimore, Maryland, USA
[3]Atmospheric Chemistry and Dynamics Laboratory, NASA Goddard Space Flight Center, Greenbelt, Maryland, USA
[4]Cooperative Institute for Research in Environmental Sciences, University of Colorado Boulder, Boulder, Colorado, USA
[5]Chemical Sciences Division, NOAA Earth System Research Laboratory, Boulder, Colorado, USA
[6]Department of Chemistry and Biochemistry, University of Colorado, Boulder, Colorado, USA
[7]Department of Earth and Planetary Sciences, Harvard University, Cambridge, Massachusetts, USA
[8]School of Engineering and Applied Sciences, Harvard University, Cambridge, Massachusetts, USA
[a]now at: School of Environmental Science and Engineering, Gwangju Institute for Science and Technology, Gwangju, Korea
[b]now at: School of Engineering and Applied Sciences and Department of Chemistry and Chemical Biology, Harvard University, Cambridge, Massachusetts, USA

Correspondence to: J. Kaiser (jen.b.kaiser@gmail.com)

Received: 31 January 2015 – Published in Atmos. Chem. Phys. Discuss.: 04 March 2015
Revised: 12 June 2015 – Accepted: 01 July 2015 – Published: 13 July 2015

Abstract. The yield of formaldehyde (HCHO) and glyoxal (CHOCHO) from oxidation of volatile organic compounds (VOCs) depends on precursor VOC structure and the concentration of NO_x ($NO_x = NO + NO_2$). Previous work has proposed that the ratio of CHOCHO to HCHO (R_{GF}) can be used as an indicator of precursor VOC speciation, and absolute concentrations of the CHOCHO and HCHO as indicators of NO_x. Because this metric is measurable by satellite, it is potentially useful on a global scale; however, absolute values and trends in R_{GF} have differed between satellite and ground-based observations. To investigate potential causes of previous discrepancies and the usefulness of this ratio, we present measurements of CHOCHO and HCHO over the southeastern United States (SE US) from the 2013 SENEX (Southeast Nexus) flight campaign, and compare these measurements with OMI (Ozone Monitoring Instrument) satellite retrievals. High time-resolution flight measurements show that high R_{GF} is associated with monoterpene emissions, low R_{GF} is associated with isoprene oxidation, and emissions associated with oil and gas production can lead to small-scale variation in regional R_{GF}. During the summertime in the SE US, R_{GF} is not a reliable diagnostic of anthropogenic VOC emissions, as HCHO and CHOCHO production are dominated by isoprene oxidation. Our results show that the new CHOCHO retrieval algorithm reduces the previous disagreement between satellite and in situ R_{GF} observations. As the absolute values and trends in R_{GF} observed during SENEX are largely reproduced by OMI observations, we conclude that satellite-based observations of R_{GF} can be used alongside knowledge of land use as a global diagnostic of dominant hydrocarbon speciation.

1 Introduction

Though volatile organic compounds (VOCs) are present only in trace amounts in the atmosphere, their presence can drive the formation of pollutants such as secondary organic aerosol and ozone. The impact of VOC emissions on tropospheric chemistry depends on the speciation of emitted VOCs and their degradation pathways. As many as 10^5 different species of VOCs are estimated to have been measured in the atmo-

sphere (Goldstein and Galbally, 2007). While an air mass will usually contain a large variety of VOCs, often a particular species or subset of species (e.g., biogenics) will dominate the photochemistry, giving rise to the production of a range of oxygenated VOCs (OVOCs). Thus, OVOCs can provide downstream constraints on the rates and pathways of VOC oxidation.

Here, we focus on the production of two ubiquitous OVOCs: formaldehyde (HCHO) and glyoxal (CHOCHO). HCHO is formed from the oxidation of nearly every anthropogenic and biogenic VOC (AVOC/BVOC, respectively). Though photochemical formation is thought to dominate the HCHO global budget (Fortems-Cheiney et al., 2012), direct HCHO emissions from pyrogenic, anthropogenic, and biogenic activity have also been observed (Guenther et al., 1995; Kesselmeier et al., 1997; Holzinger et al., 1999; Garcia et al., 2006; DiGangi et al., 2011). CHOCHO is formed from the oxidation of a smaller subset of VOCs, particularly alkenes, aromatics, isoprene, and monoterpenes (Fu et al., 2008). Direct emission from biofuel and biomass burning can also be a significant source of CHOCHO (McDonald et al., 2000; Hays et al., 2002; Christian et al., 2003; Greenberg et al., 2006). Because the yields of HCHO and CHOCHO differ between classes of VOC, and because their atmospheric lifetimes are similar, the relative abundance of CHOCHO and HCHO has been hypothesized to reflect the speciation of VOCs contributing to total VOC reactivity (Vrekousiss et al., 2010; DiGangi et al., 2012; MacDonald et al., 2012; Li et al., 2014; Miller et al., 2014).

A major motivating factor for examining the ratio of glyoxal to formaldehyde (R_{GF}, in units of mole mole^{-1}) is the ability to quantify both compounds on a global scale from satellite retrievals. Currently, HCHO and CHOCHO are the only two OVOCs with UV–visible absorption features strong enough to enable solar backscatter measurements of vertical column densities. Long-term continuous HCHO columns are available from four satellite-based instruments: GOME (Global Ozone Monitoring Experiment), SCIAMACHY (SCanning Imaging Absorption spectroMeter for Atmospheric CHartographY), OMI (Ozone Monitoring Instrument), and GOME-2. CHOCHO retrievals are available from SCIAMACHY, OMI, and GOME-2. Satellite-derived R_{GF} could be a promising diagnostic tool in determining the speciation of VOC precursors that lead to pollution formation in a given region, especially as retrievals improve in temporal and spatial resolution.

Table 1 summarizes previously published observations and conclusions about R_{GF}. Using GOME-2 satellite retrievals, Vrekoussis et al. (2010) observed R_{GF} as low as 3 % in anthropogenic regions and between 4 and 6 % over heavily vegetated regions. This was interpreted as an indication that anthropogenic precursors favor HCHO production relative to CHOCHO, while biogenic precursors favor CHOCHO production relative to HCHO. Primary emissions of HCHO were also thought to lower the observed R_{GF} in anthropogenic regions. In contrast, using ground-based measurements, DiGangi et al. (2012) observed R_{GF} values typically < 2 % in rural areas, while fresh anthropogenic influence increased R_{GF} to 4 %. These observations yielded a directly contradictory interpretation: AVOCs favor CHOCHO production, whereas BVOCs favor HCHO production. Furthermore, DiGangi et al. (2012) showed that, given the same VOC speciation, R_{GF} was invariant despite changes in observed NO_x concentrations. They proposed that this was a result of CHOCHO and HCHO formation primarily via the high-NO_x pathway of organic peroxy radical (RO_2) reactions, which in turn makes the absolute concentration of either OVOC equally dependant on NO_x and therefore leaves R_{GF} unchanged.

Following these two investigations, high values of R_{GF} (20–40 %) were observed above an Asian tropical forest (MacDonald et al., 2012), agreeing qualitatively with the conclusion of Vrekoussis et al. (2010) that high R_{GF} is consistent with biogenic source areas. The reported R_{GF} values, however, are an order of magnitude greater than satellite observations (Vrekoussis et al., 2010; Miller et al., 2014). Li et al. (2014) report an average R_{GF} of 6 % at a semi-rural site in southern China. Both observations and model simulations showed that increasing AVOC emissions lead to an increase in R_{GF}. The model simulations indicated R_{GF} was controlled not only by VOC speciation, but also by NO_x and OH mixing ratios, as well as physical processes such as CHOCHO deposition and aerosol uptake (Li et al., 2014). Recently, a new algorithm for the retrieval of CHOCHO from OMI was developed which lessens sensitivity to water vapor abundance and produces on average lower CHOCHO vertical column densities due to the choice of reference sector (Miller et al., 2014). In contrast to the ranges of R_{GF} reported by Vrekoussis et al. (2010), the OMI retrieval yields high R_{GF} in areas associated with monoterpene emissions, intermediate R_{GF} in areas dominated by anthropogenic emissions, and low R_{GF} in regions associated with strong isoprene emissions.

The cause of the discrepancies between satellite and ground-based R_{GF} trends and absolute values are unknown. DiGangi et al. (2012) suggested column-integrated and ground-based measurements in forests may differ due to direct HCHO emissions, and boundary layer ratios could be systematically lower than free troposphere ratios. Additionally, Miller et al. (2014) highlight interferences from water vapor, reference sector selection, and multi-year averaging as potential causes for the previous errors in satellite retrievals. Despite the different ranges and trends of observed values, all previously published work concludes that R_{GF} reflects at least in part the speciation of VOCs in a given air mass. If R_{GF} is to be used as a global tracer of VOC composition, all factors influencing R_{GF} must be fully elucidated, and satellite retrievals must be validated against field observations.

With flights transecting both anthropogenic and biogenic regions, as well as profiles extending from the boundary layer into the free troposphere, the 2013 SENEX (Southeast Nexus) field campaign provides an unprecedented opportu-

Table 1. Summary of previously published absolute values and trends of R_{GF}.

Reference	Method	R_{GF} under biogenic influence (%)	R_{GF} under anthropogenic influence (%)	Trend in R_{GF} with anthropogenic influence
Vrekousiss et al. (2010)	Satellite	> 4.5	< 4.5	Decreasing
DiGangi et al. (2012)	LIF[a]/LIP[b]; review of previous ground-based measurements	< 2	> 2.5	Increasing; independent of NO_x
MacDonald et al. (2012)	DOAS[c]; model analysis	20–40	–	–
Li et al. (2014)	DOAS; model analysis	0.2–17		Generally increasing; depends on NO_x, OH, and physical processes
Miller et al. (2014)	Satellite	< 4 (isoprene) > 4 (monoterpenes)	~ 4	Depends on BVOC
This work	LIF/ACES[d]	< 2.5(isoprene) > 3 (monoterpenes)	variable	Depends on BVOC and AVOC

[a] Laser-induced fluorescence (HCHO). [b] Laser-induced phosphorescence (CHOCHO). [c] Differential optical absorption spectroscopy. [d] Airborne cavity enhanced spectrometer (CHOCHO).

nity to address these uncertainties. Unlike ground-based field campaigns, the flight campaign provides information about the vertical structure of the trace gasses and a direct, real-time comparison of R_{GF} in urban outflow and in the surrounding rural areas. To our knowledge, this data represents the first high-time-resolution, simultaneous in situ flight-based measurements of HCHO and CHOCHO. We present absolute mixing ratios of HCHO and CHOCHO observed during daytime flights in the southeastern United States (SE US) and discuss the observed relationships of R_{GF} with observed VOC precursors and anthropogenic influence. Finally, to investigate the applicability of our findings for global studies, we compare flight-based R_{GF} values with those derived from OMI observations.

2 Experimental methods

2.1 SENEX flight measurements

During the SENEX project in June and July of 2013, HCHO, CHOCHO, NO_x, and VOC measurements were acquired simultaneously from the NOAA WP-3D research aircraft during 13 daytime flights. An in-depth description of the SENEX science goals, NOAA WP-3D aircraft, all onboard instrumentation, and each flight plan can be found elsewhere (http://www.esrl.noaa.gov/csd/projects/senex/). A summary of average conditions for each flight is provided in Table S1 in the Supplement.

HCHO was measured at 1 Hz by the NASA In Situ Airborne Formaldehyde (ISAF) instrument (Cazorla et al., 2015), which is based on the FIber Laser-Induced Fluorescence (FILIF) technique (Hottle et al., 2009; DiGangi et al., 2011; Kaiser et al., 2014). The reported accuracy of the HCHO measurements is 10 %. CHOCHO was measured at 0.2 Hz by Airborne Cavity Enhanced Spectrometer (ACES) with 6 % accuracy (Washenfelder et al., 2011). The precision of the CHOCHO measurement was a significant fraction of the typical ambient concentration (32 ppt precision, with a typical concentration of 100–150 pptv), such that precision is a more stringent limitation on data quality than accuracy relative to HCHO, for which the signal was consistently much larger (HCHO precision 25 ppt, with concentrations typically > 3 ppb).

NO and NO_2 were measured by ozone-induced chemiluminescence (CL) and UV photolysis followed by CL, respectively (Ryerson et al., 2000; Pollack et al., 2010). VOCs were measured at 20 % accuracy using proton-transfer reaction mass spectrometry (de Gouw and Warneke, 2007). Unless otherwise specified, all data shown here are filtered to remove in-cloud measurements, measurements below 200 m or above 1200 m, and data that may be affected by the exhaust of the WP-3D aircraft. R_{GF} is calculated by averaging the 1 s HCHO data to the 5 s CHOCHO observations.

2.2 Satellite retrievals

The OMI is a nadir viewing UV–visible grating spectrometer, launched onboard the NASA Aura satellite in July 2004 (Levelt et al., 2006). OMI provides daily global coverage at high spatial resolution (13×24 km footprint at nadir). We use slant column densities (Ω_s) of HCHO and CHOCHO from 2006 to 2007 derived from fits to OMI spectra (González Abad et al., 2015; Miller et al., 2014). HCHO and CHOCHO are retrieved between 328.5–365.5 and 435–461 nm, respectively. Slant columns are adjusted to vertical column densities (Ω_v) using scattering weights ($S(z)$) archived from the retrieval product, and species concentra-

tion profiles ($n(z)$) from the GEOS-Chem (Goddard Earth Observing System) chemical transport model (v9-01-03) (Bey et al., 2001; Mao et al., 2013).

$$\Omega_{\mathrm{v}} = \Omega_{\mathrm{s}} \frac{\int_0^{\infty} n(z)\,\mathrm{d}z}{\int_0^{\infty} S(z)\,n(z)\,\mathrm{d}z} \quad (1)$$

Here we use daily GEOS-Chem profiles spanning the observation period averaged between 13:00 and 14:00 local time (LT), close to the satellite equatorial crossing time (13:38 LT). The satellite observations are gridded as seasonal averages on a $0.5^\circ \times 0.5^\circ$ (lat $\times$ long) grid. In this analysis, we use the averaged vertical column densities for June–August of 2007. The overlap between the satellite footprint and output grid is accounted for using an area-weighted tessellation algorithm (Liu et al., 2006). Satellite pixels with cloud fractions larger than 0.2 (derived from the OMI O_2–O_2 cloud algorithm (Stammes et al., 2008) and those impacted by the row anomaly (http://www.knmi.nl/omi/research/product/rowanomaly-background.php) are filtered before gridding.

The sources of errors in satellite measurements are numerous, including uncertainties in temperature-dependent absorption cross sections, the computation of the air mass factor, instrumental errors (e.g., wavelength calibration), potential interferences from other compounds, and low signal to noise. Seasonal averaging helps to reduce these errors. Assuming a 15 % systematic uncertainty and following the formulation thoroughly explained in Vrekoussis et al. (2010), (Sect. 4.3.1), the average error in satellite R_{GF} over the SE US is 0.005, which is 18 % of the average R_{GF} value observed in this region.

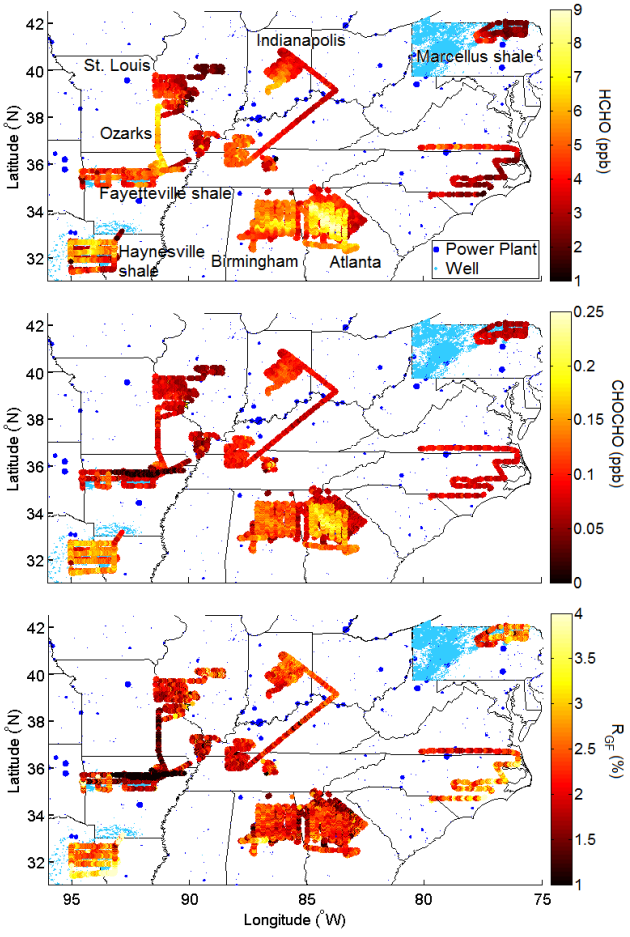

Figure 1. Daytime flight tracks colored by HCHO, CHOCHO, and R_{GF}. Power plant markers are scaled by NO_x emissions.

3 Results and discussion

Figure 1 shows daytime SENEX flight tracks colored by HCHO, CHOCHO, and R_{GF}, with major emissions sources also indicated. Emissions information was acquired from the Continuous Emissions Monitoring Systems data set for July–September of 2012 (http://ampd.epa.gov/ampd/). In general, HCHO and CHOCHO mixing ratios are higher in the areas associated with high BVOC emissions (southern flights). In particular, high HCHO is observed over the Ozarks "isoprene volcano" (Wiedinmyer et al., 2005). The concentrations of both OVOCs are higher in regions with anthropogenic influence than in the surrounding biogenically dominated areas. Compared to the northern cities of Indianapolis and St. Louis, Birmingham and Atlanta have higher mixing ratios of HCHO and CHOCHO in their outflows. The Haynesville shale region has higher mixing ratios of both OVOCs, and CHOCHO is especially enhanced. While HCHO and CHOCHO mixing ratios each vary by more than a factor of 4, the overall variability of R_{GF} observed during the SENEX flight campaign is low.

Boundary HCHO and CHOCHO measurements were also acquired during the Nashville/Middle Tennessee Ozone Study in June/July of 1995. While the SENEX flight tracks more heavily sampled oil and natural gas fields, both studies are mainly representative of the isoprene-rich SE US. The average HCHO mixing ratio is similar (4.2 ppb in 1995, 4.4 ppb in this study), as is the average CHOCHO mixing ratio (0.07 ppb in 1995, 0.10 ppb in this study), leading to similar R_{GF} (1.7 % in 1995, 2.2 % in this study) (Lee et al., 1998).

Figure 2 shows the same SENEX flight data gridded to the resolution of the OMI satellite retrievals ($0.5^\circ \times 0.5^\circ$). Removing the flights with distinctly high or low R_{GF} observations (10, 25, and 26 June), the average gridded R_{GF} is $2.5\,\% \pm 0.5\,\%$, with a correlation coefficient between HCHO and CHOCHO of $r^2 = 0.70$. Below, we discuss these regions of notably high and low R_{GF} as well as the influence of urban emissions on the ratio.

Variability in the time of measurement may have an impact on the comparison of absolute concentrations of both OVOCs and R_{GF}, as measurements were acquired over a range of

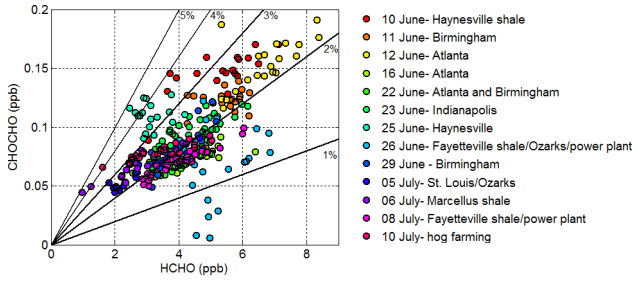

Figure 2. The relationship of CHOCHO and HCHO for each flight, gridded to OMI satellite resolution. Flights with extreme values of R_{GF} include those to the Haynesville shale (10 and 25 June) and the Ozarks (26 June).

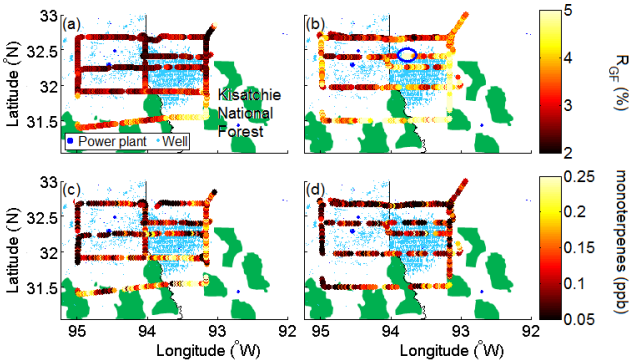

Figure 3. Flight tracks for 10 June **(a, c)** and 25 June **(b, d)** over the Haynesville shale, colored by R_{GF} and the measured monoterpene mixing ratio. The southeast corner highlights high R_{GF} in a region with high monoterpene concentrations. The blue circle indicates the location of high R_{GF} discussed further in the text. Figure 5 shows meteorological and trace gas measurements acquired at this location. National parks are shown in green, and the Kisatchie National Forest is labeled in **(a)**.

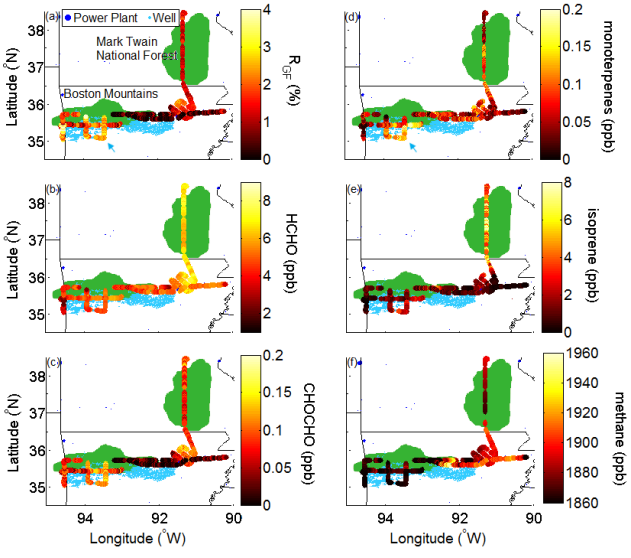

Figure 4. Flight track for 26 June over the Fayetteville shale, the independence power plant, and the Ozarks, colored by the specified trace gas mixing ratio and R_{GF}. The blue arrow highlights the region of elevated monoterpene mixing ratios. National forests are shown in green.

mid-day hours (∼ 10:00–17:00 LT; see Table S1), and both HCHO and CHOCHO have strong diurnal cycles. By comparing the observations made within 1 h on the same day, we aim to minimize any impact that diurnal variation of R_{GF} would have on this analysis.

3.1 Regions of high R_{GF}

During flights on 10 and 25 June, the region responsible for the high observed R_{GF} (4–7 %) is in the southeast corner of the flight track, over the Kisatchie National Forest (Fig. 3a, b). The dominant tree species in this region is longleaf pine (http://www.wlf.louisiana.gov). Longleaf pine (*Pinus palustris*) is reported to emit monoterpenes but not isoprene (Rasmussen, 1972). The measured emission rate of β-pinene is the largest, and approximately 30 % greater than the α-pinene emission rate. All other monoterpene emission rates are at least an order of magnitude lower (Geron et al., 2000). Indeed, measured monoterpene mixing ratios are elevated over this portion of the flight track (Fig. 3c, d), while isoprene (not shown) is relatively constant over the footprints of both flights. The high-monoterpene/high-R_{GF} relationship is in agreement with the Miller et al. (2014) satellite observation of high R_{GF} values above the boreal forests, where the high CHOCHO yield of monoterpenes is cited as the primary driver of R_{GF} (Fu et al., 2008). As in the two flights over the Kisatchie Forest, the 26 June flight also highlights a region with high monoterpenes and $R_{GF} > 3$ % (arrow in Fig. 4).

Also on the 25 June flight, high R_{GF} (> 8 %) is seen on the northeast side of the flight track (circled in Fig. 3b and d). Unlike the high R_{GF} associated with the monoterpene emissions, these values are not replicated in the same area during the 10 June flight. In this region, R_{GF} is driven by a decrease in HCHO mixing ratio while the CHOCHO mixing ratio is slightly elevated (Fig. 5). Sharp features in meteorological measurements such as potential temperature, an increase in ozone, and a decrease in all other VOC and OVOC mixing ratios suggest an incursion of free tropospheric air. Given the lack of VOC precursors and other oxidation products, and assuming it is not a measurement artifact, the source of CHO-CHO in the free troposphere is still unknown. The effect of trace gas vertical profile structure on the analysis of R_{GF} is examined in further detail in Sect. 3.4.

3.2 Regions of low R_{GF}

On the 26 June flight, north of the gas production near the eastern side of the flight track, CHOCHO concentrations are low while HCHO mixing ratios are typical of other SENEX observations, driving R_{GF} to near 0 % (Fig. 4). Concentra-

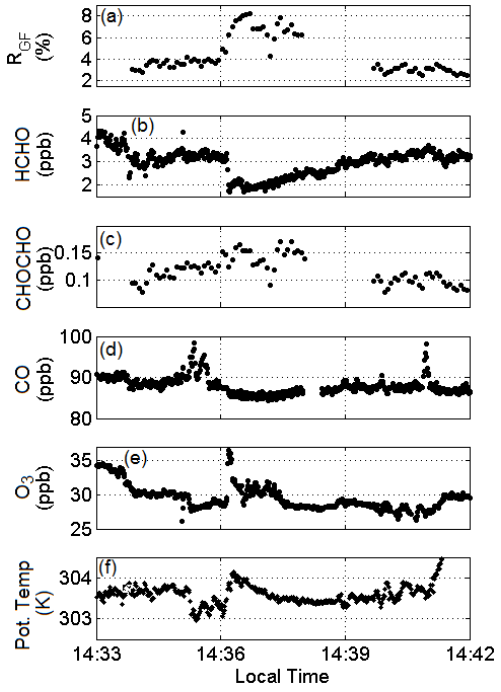

Figure 5. Time series of specified measurements during the rapid increase in R_{GF} observed south of Shreveport on the 25 June flight (blue circle in Fig. 3). An incursion of free tropospheric air near 14:36 LT drives high R_{GF}.

tions of BVOC and AVOC precursors are also low in this region; however, methane mixing ratios are dramatically elevated. While isoprene is the dominant VOC in terms of calculated OH reactivity, increased HCHO relative to CHOCHO could be a result of oxidation of alkanes, which are associated with oil and natural gas (O&NG) production (Gilman et al., 2013). Gas flaring could also be a large source of direct HCHO emissions (Pikelnaya et al., 2013).

On the portion of the 26 June flight flown over the Mark Twain National Forest in the Missouri Ozarks (Fig. 4), the average R_{GF} is 1.1 ± 0.2 %. Here, the average isoprene concentration is high (7 ± 2 ppb), NO_x is low (0.23 ± 0.02 ppb), and AVOC concentrations are low compared to BVOCs (toluene $= 0.06 \pm 0.01$ ppb). This suggests relatively pristine regions with strong isoprene emissions can be characterized by low R_{GF}. It is important to note that these measurements were acquired later in the day than most other measurements ($\sim$ 02:30 LT, Table S1), and approximately 3 h later than the measurements acquired on the southwest portion of the flight track. We thus cannot rule out diurnal variation as an influence on R_{GF} in this region.

3.3 Urban influence on R_{GF}

Because R_{GF} may be influenced by AVOC emissions and/or NO_x (Table 1), it has been proposed that R_{GF} can be used as a diagnostic of the chemistry that leads to O_3 formation

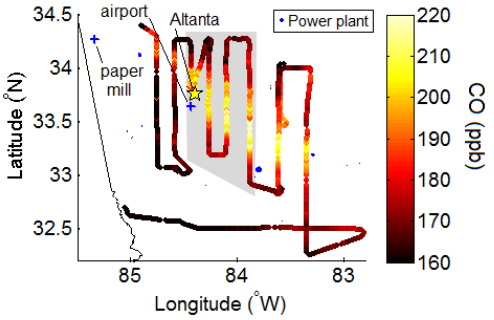

Figure 6. Flight track for 12 June colored by CO, which shows the combined outflow of Atlanta, the airport, and a paper mill on the surrounding background. Measurements acquired in the shaded area are shown in Fig. 7.

(Vrekousiss et al., 2010; DiGangi et al., 2012; Li et al., 2014). Potential explanations for varying R_{GF} in urban areas include (1) preferential formation of one OVOC from AVOCs, (2) faster oxidation caused by high OH leading to different relative concentrations of the OVOCs, and (3) differing NO_x dependencies of OVOC yields.

A comparison of in-plume and surrounding background measurements from the 12 June flight through Atlanta can help determine which of these factors may contribute to differences in observed R_{GF}. During this flight, northwesterly winds brought emissions from a nearby paper mill and power plant over the Atlanta area. As it traveled, the plume encountered emissions from the Atlanta international airport and other point and area sources. Figure 6 shows the flight path colored by CO, which demonstrates the boundary between background and polluted air. Figure 7 shows the mixing ratios of isoprene, toluene, NO_x, HCHO, CHOCHO, and the observed R_{GF} for the first four transects downwind of Atlanta.

Inside the plume, NO_x is enhanced, AVOCs such as toluene are high, BVOC mixing ratios are low, and concentrations of both OVOCs increased significantly (Fig. 7). However, no clear distinction between in-plume and background measurements can be seen in R_{GF}. This trend in increasing HCHO and CHOCHO but consistent R_{GF} is also seen in several other flight tracks following urban outflow (for further examples see Figs. S1 and S2 in the Supplement highlighting the 5 July flight over St. Louis).

There are two potentially compounding causes of the increase in HCHO and CHOCHO concentrations. First, direct emissions of the OVOCs or oxidation of AVOCs in the plume add to the background concentrations of HCHO and CHOCHO. While the oxidation of the observed AVOCs will increase OVOCs, the contribution of isoprene and its first-generation oxidation products methyl vinyl ketone (MVK) and methacrolein (MACR) to OH reactivity is more than 10 times greater than the contribution from measured AVOCs. Therefore, isoprene is still likely the dominant HCHO

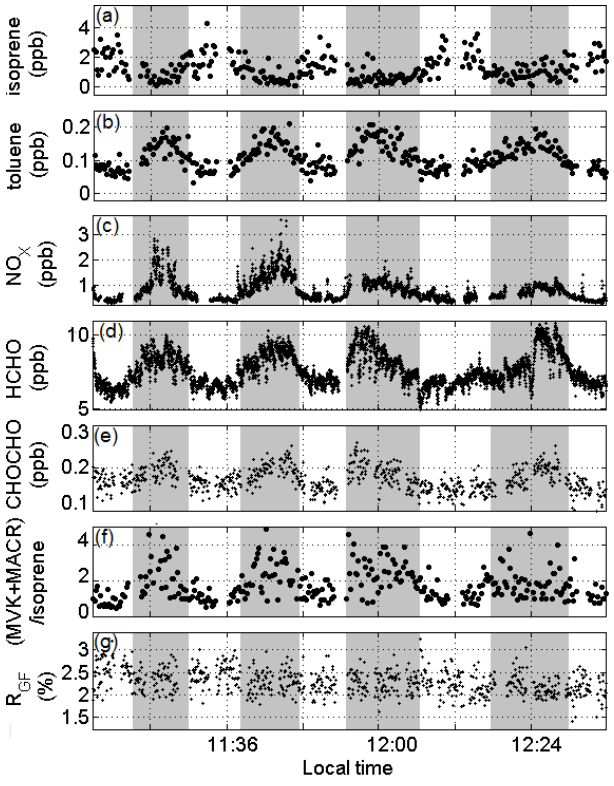

Figure 7. Measurements acquired on the 12 June flight corresponding to the boxed in region in Fig. 6. Shaded regions indicate high anthropogenic influence. While the measurements alter between AVOC/high NO_x and BVOC/low NO_x regimes, little change is seen in R_{GF}. The maximum values of NO_x and (MVK + MACR) / isoprene fall above the limits shown here.

and CHOCHO precursor. Second, higher NO_x in the plume leads to more efficient oxidation of VOCs, depleting mixing ratios of primary VOCs such as isoprene and increasing its oxidation products. This is consistent with the classical NO_x dependence of OH concentrations (Rohrer et al., 2014). The ratio of MVK and MACR to isoprene can be used as an indicator of the extent of photochemical processing (Fig. 7). The higher in-plume ratio of MVK + MACR to isoprene supports the conclusion that oxidation occurs faster in the plume. It is important to note that the low-NO_x oxidation product ISOPOOH (isoprene hydroxy hydroperoxide) can interfere with PTR-MS (proton-transfer reaction mass spectrometry) measurements of MVK + MACR (Rivera-Rios et al., 2014), and potentially also measurements of HCHO. If ISOPOOH creates a positive bias MVK + MACR measurement, the artifact would be larger in the low-NO_x areas, artificially increasing the (MVK + MACR) / isoprene ratio observed outside of the plume. Because (MVK + MACR) / isoprene is higher inside the plume, any interference would not affect the conclusion that oxidation occurs faster in the plume.

The absolute concentrations of HCHO and CHOCHO point to more rapid oxidation of isoprene in-plume as well as a potentially small contribution of AVOCs to both overall OVOC budgets, but neither of these characteristics influence R_{GF}. As stated above, a third potential driver of R_{GF} is a difference in high- and low-NO_x oxidation mechanisms. Again, though the NO_x concentrations observed in-plume are significantly different than the surrounding air such that RO_2 spans different fates (reaction with NO versus reaction with HO_2 and isomerization), no characteristic change in R_{GF} is observed. Therefore, R_{GF} cannot be used to diagnose AVOC emissions, RO_2 fate, or OH levels in urban areas where isoprene emissions dominate the HCHO and CHOCHO budgets.

As discussed in Sect. 3.2, the Ozarks demonstrated especially low R_{GF}. Both the Atlanta background air and the Ozarks are low-NO_x isoprene-dominated regions (0.5 ppb NO_x near Atlanta, 0.2 ppb NO_x in the Ozarks), yet R_{GF} observations in these areas are significantly different. As previously discussed, urban emissions do not cause significant changes in R_{GF} if isoprene is the dominant VOC; therefore, some other factor must contribute to the comparably low R_{GF} over the Ozarks. While the observations of R_{GF} over the Ozarks were acquired at ∼ 14:20 LT, later observations of R_{GF} in the plume background are not significantly different than the earlier observations shown in Fig. 7 (R_{GF} of 2.2 ± 0.3 % between 14:00 and 14:30 LT). This suggests that diurnal variation of R_{GF} is not the driving cause of the difference between Atlanta and Ozark observations.

The most notable difference between the regions is the observed concentrations of isoprene. Isoprene reached over 10 ppb in the Ozarks, while the Atlanta background air reached only 4 ppb. A stronger relative contribution of monoterpenes to the HCHO and CHOCHO budgets in Atlanta could result in the higher observed R_{GF} (∼ 50 ppt monoterepene per pbb isoprene near Atlanta, ∼ 15 ppt monoterepene per ppb isoprene near the Ozarks). Alternatively, the relationship of HCHO and CHOCHO with isoprene may be non-linear, with higher isoprene emissions leading to lower R_{GF}. Because low-NO_x isoprene oxidation is not well understood, especially with respect to OH concentrations (Rohrer et al., 2014), HCHO yields (Palmer et al., 2006; Marais et al., 2012), and CHOCHO yields (Stavrakou et al., 2009), model analysis cannot conclusively determine the cause of decreasing R_{GF} with increasing isoprene emissions. A model can be useful, however, in determining the anticipated influence of hydrocarbon speciation on R_{GF}, as discussed below.

3.4 Modeled trends in R_{GF} with hydrocarbon speciation

The values of R_{GF} presented above suggest that (1) monoterpene oxidation leads to higher R_{GF} than isoprene, (2) AVOCs must have substantially high concentrations to affect R_{GF} in regions with high isoprene emissions, and (3) depending on the surrounding BVOC emissions, alkanes could decrease

Table 2. Relative abundance of HCHO and CHOCHO from 1 ppb of a given precursor[a].

Precursor	CHOCHO	HCHO	Ratio (%)[b]
Isoprene	0.27 ppb	4.3 ppb	6.3
α-pinene	0.31 ppb	3.6 ppb	8.6
β-pinene	0.49 ppb	3.6 ppb	14
Ethane	0.02 ppt	5.4 ppt	0.4
Ethene	586 ppt	24 ppt	4.2
Ethyne	0.91 ppt	14 ppt	1500
Propane	0.02 ppt	8.8 ppt	0.2
n-butane	1.5 ppt	140 ppt	1.1
Benzene	23 ppt	7.6 ppt	303
Toluene	103 ppt	150 ppt	69

[a] Calculated using a 0-D box model. See text for details.
[b] Ratio = CHOCHO / HCHO.

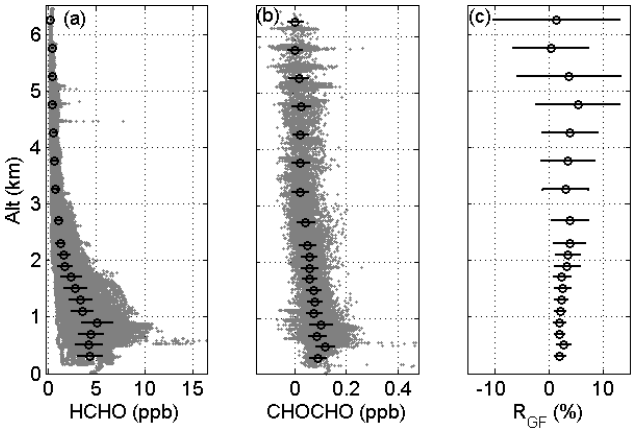

Figure 8. Average vertical profile of **(a)** HCHO and **(b)** CHOCHO measurements acquired during the flights specified in Fig. 1. Gray dots represent all measurements, black circles are averages in a given altitude bin, and error bars are standard deviation within that bin. Bins are 200 m in height from 200 to 2500 m, and 500 m thereafter. **(c)** R_{GF} calculated from average HCHO and CHOCHO profiles. Error bars are calculated from the standard deviations of HCHO and CHOCHO observations.

the regional R_{GF}. To examine if these results are consistent with our understanding of the oxidation mechanisms of each VOC precursor, a simple 0-D box model analysis was performed using the University of Washington Chemical Box Model (UWCM) (Wolfe and Thornton, 2011), which incorporates the Master Chemical Mechanism v 3.2 (Jenkin et al., 1997; Saunders et al., 2003).

The intent of these model scenarios is not to compare modeled concentrations of CHOCHO and HCHO to their observed values, nor to compare modeled and measured R_{GF}, but to investigate the relative values of R_{GF} predicted by the model for each VOC precursor. Temperature, relative humidity, O_3, and CO are held at their observed campaign averages (297 K, 70 %, 51, and 140 ppb, respectively). OH is held at 4×10^6 molec cm^{-3}, and NO_x is constrained to the measured values representative of the plume background on 12 June ($NO = 0.06$ ppb; $NO_2 = 0.41$ ppb). The solar zenith angle is set to 13.4°, representative of the sun's position over Atlanta at 12:00 LT on 12 June. Pressure is set to a constant 760 Torr, and all species are given an additional sink with a lifetime of 24 h in lieu of explicitly modeling physical loss processes like deposition and dilution. The only hydrocarbon present in each model scenario is the VOC of interest, held at a constant concentration of 1 ppb. Integration time is set to 5 days, at which point the concentrations of both OVOCs are nearly constant. The calculated mixing ratios of CHOCHO and HCHO at the end of the model runs are shown in Table 2.

Compared to isoprene, the two monoterpenes investigated here (α- and β-pinene) produce more CHOCHO per HCHO. As this effect has been demonstrated in model calculations, satellite observations, and flight-based measurements, we conclude that observations of high values of R_{GF} are a result of high monoterpene compared to isoprene emissions. The absolute concentrations of both OVOCs produced from the oxidation of AVOCs studied here (benzene, toluene, ethene, ethyne, and the alkanes) are substantially lower compared to the yield from BVOCs. Because these AVOCs have long lifetimes, the concentration of AVOC would need to be substantially higher than BVOC to dominate the HCHO or CHOCHO budget. This is not likely in most of the SE US. However, AVOCs can dominate chemistry in O&NG production areas (Katzenstein et al., 2003; Edwards et al., 2014) and may be relatively more important in the winter when BVOC emissions are low or in areas with less vegetation. Alkanes and ethene produce less CHOCHO per HCHO compared to all BVOCs. In contrast, ethyne, benzene, and toluene produce much more CHOCHO relative to HCHO. The effect of AVOCs on R_{GF} is likely dependent on the speciation of emitted AVOCs, the strength of local BVOC emissions, and any direct OVOC emissions (e.g., HCHO from gas flaring). These compounding factors could make measurements of R_{GF} a convoluted diagnostic for assessing the VOC composition of different air masses.

3.5 Comparison with satellite retrievals

While ideally 2013 OMI retrievals would be used in this analysis, the satellite has experienced severe degradation such that quantitative CHOCHO is not easily determined. Only the 2007 retrievals are available at this time. One of the major conclusions reached using the SENEX in situ measurements is that in the SE US, R_{GF} is not a diagnostic of anthropogenic emissions, as HCHO and CHOCHO production are dominated by isoprene oxidation. Our in situ measurements also show that R_{GF} is unaffected by NO_x and OH (Sect. 3.3). Therefore, as long as isoprene is the dominant VOC for HCHO and CHOCHO production in the SE US in both 2007 and 2013, the comparison between 2007 satel-

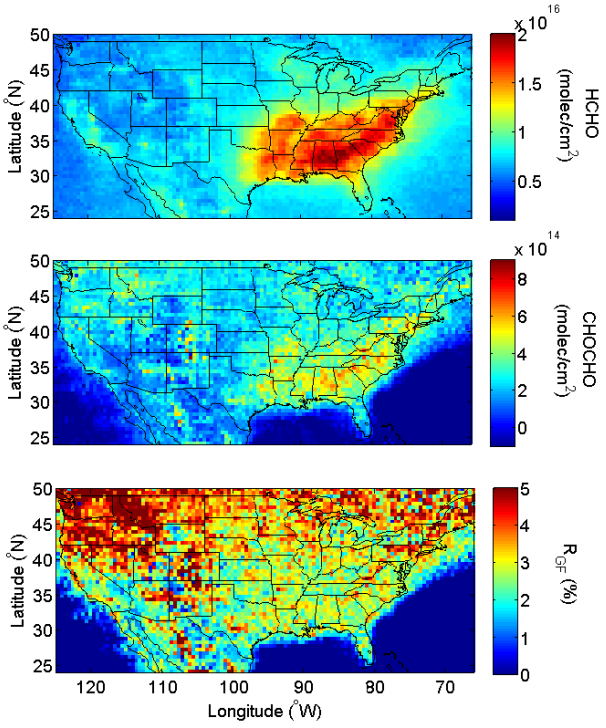

Figure 9. OMI satellite retrievals of HCHO and CHOCHO vertical density during June–August of 2007. The ratio to CHOCHO to HCHO is shown in the bottom panel.

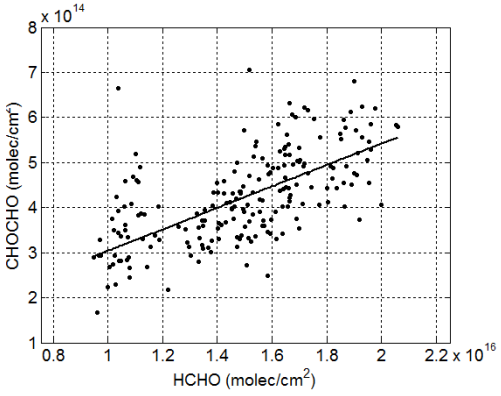

Figure 10. Satellite retrieval of CHOCHO vs. HCHO corresponding to grid coordinates of SENEX boundary layer measurements. Statistics for the linear fits are shown in Table 4.

lite and 2013 in situ R_{GF} remains valid. Both this work and analysis of the previous 1995 Nashville/Middle Tennessee Ozone Study (Lee et al., 1998) find isoprene to be the dominant HCHO source. Interannual variability of summertime isoprene emissions is estimated to be between 8 and 18 % for the contiguous US during the summers (Tawfik et al., 2012). Therefore, it is likely that isoprene is also the dominant OVOC source in 2007.

When comparing flight-based observations with satellite retrievals, it is important to consider the inherently different information these two measurements provide. Comparisons between column-integrated satellite retrievals and single-altitude measurements are only valid if the point measurements represent the seasonal mean of the behavior of the vertical column as a whole. To examine any effect of vertical distribution of HCHO and CHOCHO on satellite observations of R_{GF}, we investigate the campaign average vertical profiles of both OVOCs and R_{GF} calculated from those averages (Fig. 8). Both OVOCs show the expected decrease in concentration with altitude; however, the relative difference between boundary layer and free troposphere mixing ratios is greater for HCHO. This gives rise to a small increase in R_{GF} in the free troposphere. A higher free tropospheric R_{GF} was also observed in the 1995 Nashville/Middle Tennessee Ozone Study (Lee et al., 1998).

While R_{GF} is typically slightly higher in the free troposphere than the boundary layer, no clear altitude dependence in R_{GF} is observed within the boundary layer (Fig. 8c, altitudes less than 2 km, and Fig. S4 for individual profiles). In the free troposphere, CHOCHO measurements are below the detection limit (23 ppt at 3.25 km, detection limit = 32 ppt 5 s^{-1}). The observed variability in R_{GF} at high altitudes can largely be attributed to noise in the CHOCHO measurements at such low concentrations. Because the uncertainty in CHOCHO concentrations from measurement precision is typically greater than that from measurement accuracy, we take measured CHOCHO − 32 ppt as the lower limit of CHOCHO as measured by ACES. If measurements are positively biased by as little as 16 ppt, which is within this range of uncertainty, corrected data would not demonstrate an increase in R_{GF} with altitude.

If the difference in HCHO and CHOCHO vertical structures is not a measurement artifact, the cause of the increase in R_{GF} in the free troposphere is unclear. VOC precursors with longer lifetimes that reach the free troposphere could preferentially form CHOCHO; however, all species of measured VOCs exhibit a similar steep decrease in concentration at high altitudes. Alternatively, the lifetimes of CHOCHO and HCHO could vary with altitude in such a way that HCHO concentrations show a more steep vertical dependence. However, this is unlikely as the photolysis and reaction with OH play nearly identical roles in the relative loss processes of the two OVOCs. Li et al. (2014) inferred different mixing layer heights for the two OVOCs. They calculated that the lifetime of isoprene was shorter than the typical boundary layer mixing time and therefore hypothesized that HCHO production happened earlier (i.e., at lower altitudes) than CHOCHO production. In contrast, we see that the boundary layer is typically uniformly mixed with respect to HCHO and CHOCHO, potentially signifying the lifetime of the two OVOCs is longer than the boundary layer mixing time. Therefore, the time dependence of HCHO and CHOCHO production is un-

Table 3. Comparison of column-integrated and boundary layer R_{GF}.

Profile number	Boundary layer R_{GF}[a]	R_{GF} calculated from in situ HCHO Ω_v and CHOCHO Ω_v	Difference[b]	Percentage of altitude range in FT[c]
1	2.7	3.2	0.6	68
2	2.2	2.6	0.4	53
3	2.7	3.4	0.7	50
4	2.0	2.1	0.1	50
5	1.7	2.1	0.4	50
6	1.9	2.2	0.3	47
7	2.4	2.2	−0.2	42
8	1.9	1.9	0.0	17
9	2.1	2.1	0.0	15
10	2.5	1.9	−0.7	15
11	2.6	2.4	−0.2	8
12	2.0	2.1	0.1	8

[a] Observed at 1 km. [b] Calculated as in $\Omega_v R_{GF}$ – boundary layer R_{GF}. [c] FT: free troposphere. Boundary layer height determined by gradient in O_3.

likely to be the underlying cause of the difference in R_{GF} observed in the free troposphere. Finally, heterogeneous oxidation of aerosols has been proposed as a source of CHOCHO and other OVOCs in the free troposphere (Volkamer et al., 2015). No specific source of sufficient magnitude has been identified but processes which release glyoxal, such as the ozonolysis of fatty acids (Zhou et al., 2014), would be potential candidates. Any such source would need to produce glyoxal in excess over formaldehyde.

Regardless of the cause of the higher relative R_{GF} in the free troposphere, because the boundary layer contains the majority of HCHO and CHOCHO, the R_{GF} calculated from in situ HCHO and CHOCHO vertical column densities is only slightly higher than the average R_{GF} observed in the boundary layer (2.7 % calculated from Ω_v, 2.0 % at 900 m). A similar analysis using each local vertical profile measurement rather than the campaign average vertical profiles yields the same conclusions. Table 3 lists the R_{GF} observed in the boundary layer and the R_{GF} calculated from in situ HCHO and CHOCHO vertical column densities for all profiles extending above 3 km, which were all flown in the Atlanta–Birmingham area. A map of profile locations, HCHO and CHOCHO measurements, and R_{GF} for each profile can be found in the supporting information (Figs. S3, S4). In general, profiles with a smaller percentage of measurements acquired in the free troposphere do not display a large difference between boundary layer and R_{GF} calculated from in situ HCHO and CHOCHO vertical column densities. Individual profile measurements and campaign-averaged data support the conclusion that R_{GF} as observed by satellite retrievals should exhibit similar ranges as boundary layer observations, though a positive bias may be observed due to relatively higher CHOCHO in the free troposphere.

OMI satellite observations from June–August of 2007 over the United States are shown in Fig. 9. HCHO and CHOCHO are elevated over the SE US, where high isoprene emissions are expected to lead to increases in both OVOCs. Compared to the rest of the US, R_{GF} in this region is low. The northwest region of the US, where monoterpene emissions are high (Sakulyanontvittaya et al., 2008), demonstrates the highest R_{GF} over the US.

Table 4. Linear fits of CHOCHO vs. HCHO observations[a].

Method	Slope	Intercept	r^2	Average R_{GF} (%)
Flight	0.017	0.019 ppb	0.43	2.2
Satellite	0.024	∼ 0.016 ppb[b] (6.6×10^{13} molec cm^{-2})	0.38	2.8

[a] All data are gridded to 0.5° × 0.5° resolution for orthogonal distance regression analysis. For SENEX flight observations, all flights (including Haynesville and Fayetteville areas) are included. [b] Ground level mixing ratio was calculated assuming CHOCHO and HCHO are contained within a well-mixed 1500 m boundary layer and an atmospheric-scale height of 7.5 km.

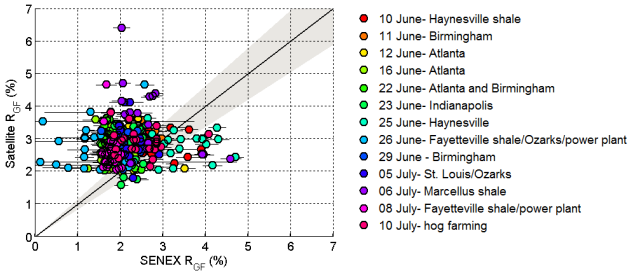

Figure 11. Satellite and SENEX R_{GF}. The line represents a 1–1 relationship, error bars represent standard deviations of SENEX measurements within the given pixel, and the shaded area represents the accuracy of the SENEX measurements.

To compare satellite and flight-based observations, flight data were averaged to the 0.5° × 0.5° OMI resolution. Summertime satellite retrievals and flight observations of CHOCHO vs. HCHO show similar correlations, with $r^2 \sim 0.4$ (Fig. 10, Table 4). The satellite average R_{GF} is ∼ 0.6 percentage points higher than flight-based observations gridded to the same resolution. While this cannot be explained by the error and standard deviation of the gridded SENEX data and the uncertainty in the vertical column densities, this percentage is much smaller than the previous discrepancies between satellite and point-based measurements (DiGangi et al., 2012).

Figure 11 shows that while there is no correlation between satellite and flight R_{GF} ($r^2 = 0.003$), the range of observed values are in good agreement (1.5–4 %). Seasonal averages of R_{GF} from satellite retrievals are less likely to reflect extreme values and high-emission events compared to flight data; therefore, high correlation is not anticipated at this timescale. Similarly, the correlations between satellite and ground HCHO ($r^2 = 0.15$) and CHOCHO ($r^2 = 0.044$) are low. Satellite and flight HCHO observations show stronger correlation than CHOCHO observations likely because CHOCHO aircraft measurements and satellite retrievals have higher relative uncertainties than HCHO retrievals (Miller et al., 2014; González Abad et al., 2015), and in situ CHOCHO measurements are close to the detection limit. The high and low values of R_{GF} observed during the

SENEX field campaign (25 and 26 June flights) are not reproduced in the satellite observations. A comparison of average BVOC emissions and O&NG production activity during the summer of 2007 and June 2013 would be needed to demonstrate that satellite R_{GF} would be expected to show similar deviations from its average value. Furthermore, small-scale variation in satellite R_{GF} is mostly associated with noise, such that retrievals shown cannot distinguish the local influences (i.e., the Kisatchie National forest).

Besides the new CHOCHO retrieval method, one key distinction between this comparison and comparisons in previous studies (i.e., DiGangi et al., 2012) is the use of satellite retrievals for only the summer observational period rather the annual averages. Ground- and flight-based measurements are typically performed in the summer, when BVOC emissions are high. Therefore, point-based measurements may be biased to display the influence of BVOC emissions on R_{GF}.

4 Conclusions: Can R_{GF} be used as a global indicator of VOC speciation?

Overall, the flight-based measurements presented here show that R_{GF} is indicative of VOC speciation in select situations. High R_{GF} ($> 3\,\%$) is consistently observed in areas with high monoterpene emissions, and low R_{GF} ($< 2.5\,\%$) is associated with strong isoprene emissions. No consistent influence of AVOC or NO_x emissions on the background R_{GF} was observed, likely because biogenic VOC emission strength determines R_{GF} in the SE US. The previously observed quick and short (2–5 min) increase in R_{GF} in DiGangi et al. (2012) may have been a result of extremely fresh emissions (e.g., diesel trucks emit at a rate of CHOCHO / HCHO = 9.4 %; Schauer et al., 1999), and not indicative of larger-scale changes in dominant VOC speciation. Emissions associated with oil and gas production areas can cause R_{GF} to deviate from the values observed over their background levels. However, the absolute value of R_{GF} in such regions is likely dependent on background BVOC emissions, speciation of AVOCs, and any direct OVOC emissions.

Compared to previous literature, absolute values of flight-based R_{GF} are in better agreement with satellite observations using the new CHOCHO retrieval algorithms. While time resolution plays a large role in direct comparisons of point-based measurements and satellite retrievals, the trend of high R_{GF} over areas with monoterpenes and low R_{GF} over areas with isoprene is broadly in agreement for the two platforms. With these trends validated by ground measurements, R_{GF} based on satellite retrievals may be useful as a diagnostic of BVOC emissions. As these retrievals become available at higher time and spatial resolutions, R_{GF} can be used to help identify the speciation of VOCs leading to secondary pollutant formation on a regional scale.

The Supplement related to this article is available online at doi:10.5194/acp-15-7571-2015-supplement.

Acknowledgements. The authors would like to acknowledge the contribution from all members of the SENEX flight and science teams. Funding was provided by US EPA Science to Achieve Results (STAR) program grant 83540601. This research has not been subjected to any EPA review and therefore does not necessarily reflect the views of the agency, and no official endorsement should be inferred. J. Kaiser acknowledges support from NASA Headquarters under the NASA Earth and Space Science Fellowship Program – grant NNX14AK97H. This work was also supported as part of the NASA Aura Science Team.

Edited by: R. McLaren

References

Bey, I., Jacob, D. J., Yantosca, R. M., Logan, J. A., Field, B. D., Fiore, A. M., Li, Q. B., Liu, H. G. Y., Mickley, L. J., and Schultz, M. G.: Global modeling of tropospheric chemistry with assimilated meteorology: Model description and evaluation, J. Geophys. Res.-Atmos., 106, 23073–23095, doi:10.1029/2001jd000807, 2001.

Cazorla, M., Wolfe, G. M., Bailey, S. A., Swanson, A. K., Arkinson, H. L., and Hanisco, T. F.: A new airborne laser-induced fluorescence instrument for in situ detection of formaldehyde throughout the troposphere and lower stratosphere, Atmos. Meas. Tech., 8, 541–552, doi:10.5194/amt-8-541-2015, 2015.

Christian, T. J., Kleiss, B., Yokelson, R. J., Holzinger, R., Crutzen, P. J., Hao, W. M., Saharjo, B. H., and Ward, D. E.: Comprehensive laboratory measurements of biomass-burning emissions: 1. Emissions from Indonesian, African, and other fuels, J. Geophys. Res., 108, 4719, doi:10.1029/2003jd003704, 2003.

de Gouw, J. and Warneke, C.: Measurements of volatile organic compounds in the earths atmosphere using proton-transfer-reaction mass spectrometry, Mass Spectrom. Rev., 26, 223–257, doi:10.1002/mas.20119, 2007.

DiGangi, J. P., Boyle, E. S., Karl, T., Harley, P., Turnipseed, A., Kim, S., Cantrell, C., Maudlin III, R. L., Zheng, W., Flocke, F., Hall, S. R., Ullmann, K., Nakashima, Y., Paul, J. B., Wolfe, G. M., Desai, A. R., Kajii, Y., Guenther, A., and Keutsch, F. N.: First direct measurements of formaldehyde flux via eddy covariance: implications for missing in-canopy formaldehyde sources, Atmos. Chem. Phys., 11, 10565–10578, doi:10.5194/acp-11-10565-2011, 2011.

DiGangi, J. P., Henry, S. B., Kammrath, A., Boyle, E. S., Kaser, L., Schnitzhofer, R., Graus, M., Turnipseed, A., Park, J-H., Weber, R. J., Hornbrook, R. S., Cantrell, C. A., Maudlin III, R. L., Kim, S., Nakashima, Y., Wolfe, G. M., Kajii, Y., Apel, E.C., Goldstein, A. H., Guenther, A., Karl, T., Hansel, A., and Keutsch, F. N.: Observations of glyoxal and formaldehyde as metrics for the anthropogenic impact on rural photochemistry, Atmos. Chem. Phys., 12, 9529–9543, doi:10.5194/acp-12-9529-2012, 2012.

Edwards, P. M., Brown, S. S., Roberts, J. M., Ahmadov, R., Banta, R. M., deGouw, J. A., Dube, W. P., Field, R. A., Flynn, J. H.,

Gilman, J. B., Graus, M., Helmig, D., Koss, A., Langford, A. O., Lefer, B. L., Lerner, B. M., Li, R., Li, S.-M., McKeen, S. A., Murphy, S. M., Parrish, D. D., Senff, C. J., Soltis, J., Stutz, J., Sweeney, C., Thompson, C. R., Trainer, M. K., Tsai, C., Veres, P. R., Washenfelder, R. A., Warneke, C., Wild, R. J., Young, C. J., Yuan, B., and Zamora, R.: High winter ozone pollution from carbonyl photolysis in an oil and gas basin, Nature, 514, 351–354, 10.1038/nature13767, 2014.

Fortems-Cheiney, A., Chevallier, F., Pison, I., Bousquet, P., Saunois, M., Szopa, S., Cressot, C., Kurosu, T. P., Chance, K., and Fried, A.: The formaldehyde budget as seen by a global-scale multi-constraint and multi-species inversion system, Atmos. Chem. Phys., 12, 6699–6721, doi:10.5194/acp-12-6699-2012, 2012.

Fu, T.-M., Jacob, D. J., Wittrock, F., Burrows, J. P., Vrekoussis, M., and Henze, D. K.: Global budgets of atmospheric glyoxal and methylglyoxal, and implications for formation of secondary organic aerosols, J. Geophys. Res.-Atmos., 113, D15303, doi:10.1029/2007jd009505, 2008.

Garcia, A. R., Volkamer, R., Molina, L. T., Molina, M. J., Samuelson, J., Mellqvist, J., Galle, B., Herndon, S. C., and Kolb, C. E.: Separation of emitted and photochemical formaldehyde in Mexico City using a statistical analysis and a new pair of gas-phase tracers, Atmos. Chem. Phys., 6, 4545–4557, doi:10.5194/acp-6-4545-2006, 2006.

Geron, C., Guenther, A., Sharkey, T., and Arnts, R. R.: Temporal variability in basal isoprene emission factor, Tree Physiol., 20, 799–805, doi:10.1093/treephys/20.12.799, 2000.

Gilman, J. B., Lerner, B. M., Kuster, W. C., and de Gouw, J. A.: Source Signature of Volatile Organic Compounds from Oil and Natural Gas Operations in Northeastern Colorado, Environ. Sci. Technol., 47, 1297–1305, doi:10.1021/es304119a, 2013.

Goldstein, A. H. and Galbally, I. E.: Known and unexplored organic constituents in the earth's atmosphere, Environ. Sci. Technol., 41, 1514–1521, doi:10.1021/es072476p, 2007.

González Abad, G., Liu, X., Chance, K., Wang, H., Kurosu, T. P., and Suleiman, R.: Updated Smithsonian Astrophysical Observatory Ozone Monitoring Instrument (SAO OMI) formaldehyde retrieval, Atmos. Meas. Tech., 8, 19–32, doi:10.5194/amt-8-19-2015, 2015.

Greenberg, J. P., Friedli, H., Guenther, A. B., Hanson, D., Harley, P., and Karl, T.: Volatile organic emissions from the distillation and pyrolysis of vegetation, Atmos. Chem. Phys., 6, 81–91, doi:10.5194/acp-6-81-2006, 2006.

Guenther, A., Hewitt, C. N., Erickson, D., Fall, R., Geron, C., Graedel, T., Harley, P., Klinger, L., Lerdau, M., McKay, W. A., Pierce, T., Scholes, B., Steinbrecher, R., Tallamraju, R., Taylor, J., and Zimmerman, P.: A global model of natural volatile compound emissions, J. Geophys. Res.-Atmos., 100, 8873–8892, doi:10.1029/94jd02950, 1995.

Hays, M. D., Geron, C. D., Linna, K. J., Smith, N. D., and Schauer, J. J.: Speciation of gas-phase and fine particle emissions from burning of foliar fuels, Environ. Sci. Technol., 36, 2281–2295, doi:10.1021/es0111683, 2002.

Holzinger, R., Warneke, C., Hansel, A., Jordan, A., Lindinger, W., Scharffe, D. H., Schade, G., and Crutzen, P. J.: Biomass burning as a source of formaldehyde, acetaldehyde, methanol, acetone, acetonitrile, and hydrogen cyanide, Geophys. Res. Lett., 26, 1161–1164, doi:10.1029/1999gl900156, 1999.

Hottle, J., Huisman, A., Digangi, J., Kammrath, A., Galloway, M., Coens, K., and Keutsch, F.: A Laser Induced Fluorescence-Based Instrument for In-Situ Measurements of Atmospheric Formaldehyde, Environ. Sci. Technol., 43, 790–795, doi:10.1021/es801621f, 2009.

Jenkin, M., Saunders, S., and Pilling, M.: The tropospheric degradation of volatile organic compounds: A protocol for mechanism development, Atmos. Environ., 31, 81–104, doi:10.1016/S1352-2310(96)00105-7, 1997.

Kaiser, J., Li, X., Tillmann, R., Acir, I., Holland, F., Rohrer, F., Wegener, R., and Keutsch, F. N.: Intercomparison of Hantzsch and fiber-laser-induced-fluorescence formaldehyde measurements, Atmos. Meas. Tech., 7, 1571–1580, doi:10.5194/amt-7-1571-2014, 2014.

Katzenstein, A. S., Doezema, L. A., Simpson, I. J., Balke, D. R., and Rowland, F. S.: Extensive regional atmospheric hydrocarbon pollution in the southwestern United States, P. Natl. Acad. Sci. USA, 100, 11975–11979, doi:10.1073/pnas.1635258100, 2003.

Kesselmeier, J., Bode, K., Hofmann, U., Muller, H., Schafer, L., Wolf, A., Ciccioli, P., Brancaleoni, E., Cecinato, A., Frattoni, M., Foster, P., Ferrari, C., Jacob, V., Fugit, J. L., Dutaur, L., Simon, V., and Torres, L.: Emission of short chained organic acids, aldehydes and monoterpenes from *Quercus ilex* L. and *Pinus pinea* L. in relation to physiological activities, carbon budget and emission algorithms, Atmos. Environ., 31, 119–133, doi:10.1016/s1352-2310(97)00079-4, 1997.

Lee, Y. N., Zhou, X., Kleinman, L. I., Nunnermacker, L. J., Springston, S. R., Daum, P. H., Newman, L., Keigley, W. G., Holdren, M. W., Spicer, C. W., Young, V., Fu, B., Parrish, D. D., Holloway, J., Williams, J., Roberts, J. M., Ryerson, T. B., and Fehsenfeld, F. C.: Atmospheric chemistry and distribution of formaldehyde and several multioxygenated carbonyl compounds during the 1995 Nashville Middle Tennessee Ozone Study, J. Geophys. Res., 103, 22449–22462, doi:10.1029/98JD01251, 1998.

Levelt, P. F., Van den Oord, G. H. J., Dobber, M. R., Malkki, A., Visser, H., de Vries, J., Stammes, P., Lundell, J. O. V., and Saari, H.: The Ozone Monitoring Instrument, IEEE T. Geosci. Remote Sens., 44, 1093–1101, doi:10.1109/tgrs.2006.872333, 2006.

Li, X., Rohrer, F., Brauers, T., Hofzumahaus, A., Lu, K., Shao, M., Zhang, Y. H., and Wahner, A.: Modeling of HCHO and CHOCHO at a semi-rural site in southern China during the PRIDE-PRD2006 campaign, Atmos. Chem. Phys., 14, 12291–12305, doi:10.5194/acp-14-12291-2014, 2014.

Liu, X., Chance, K., Sioris, C. E., Kurosu, T. P., Spurr, R. J. D., Martin, R. V., Fu, T. M., Logan, J. A., Jacob, D. J., Palmer, P. I., Newchurch, M. J., Megretskaia, I. A., and Chatfield, R. B.: First directly retrieved global distribution of tropospheric column ozone from GOME: Comparison with the GEOS-CHEM model, J. Geophys. Res.-Atmos., 111, D02308, doi:10.1029/2005jd006564, 2006.

MacDonald, S. M., Oetjen, H., Mahajan, A. S., Whalley, L. K., Edwards, P. M., Heard, D. E., Jones, C. E., and Plane, J. M. C.: DOAS measurements of formaldehyde and glyoxal above a south-east Asian tropical rainforest, Atmos. Chem. Phys., 12, 5949–5962, doi:10.5194/acp-12-5949-2012, 2012.

Mao, J., Paulot, F., Jacob, D. J., Cohen, R. C., Crounse, J. D., Wennberg, P. O., Keller, C. A., Hudman, R. C., Barkley, M. P., and Horowitz, L. W.: Ozone and organic nitrates over the east-

ern United States: Sensitivity to isoprene chemistry, J. Geophys. Res.-Atmos., 118, 11256–11268, doi:10.1002/jgrd.50817, 2013.

Marais, E. A., Jacob, D. J., Kurosu, T. P., Chance, K., Murphy, J. G., Reeves, C., Mills, G., Casadio, S., Millet, D. B., Barkley, M. P., Paulot, F., and Mao, J.: Isoprene emissions in Africa inferred from OMI observations of formaldehyde columns, Atmos. Chem. Phys., 12, 6219–6235, doi:10.5194/acp-12-6219-2012, 2012.

McDonald, J. D., Zielinska, B., Fujita, E. M., Sagebiel, J. C., Chow, J. C., and Watson, J. G.: Fine particle and gaseous emission rates from residential wood combustion, Environ. Sci. Technol., 34, 2080–2091, doi:10.1021/es9909632, 2000.

Miller, C., Gonzalez Abad, G., Wang, H., Liu, X., Kurosu, T., Jacob, D. J., and Chance, K.: Glyoxal retrieval from the Ozone Monitoring Instrument, Atmos. Meas. Tech., 7, 3891–3907, doi:10.5194/amt-7-3891-2014, 2014.

Palmer, P. I., Abbot, D. S., Fu, T.-M., Jacob, D. J., Chance, K., Kurosu, T. P., Guenther, A., Wiedinmyer, C., Stanton, J. C., Pilling, M. J., Pressley, S. N., Lamb, B., and Sumner, A. L.: Quantifying the seasonal and interannual variability of North American isoprene emissions using satellite observations of the formaldehyde column, J. Geophys. Res.-Atmos., 111, D12315, doi:10.1029/2005jd006689, 2006.

Pikelnaya, O., Flynn, J. H., Tsai, C., and Stutz, J.: Imaging DOAS detection of primary formaldehyde and sulfur dioxide emissions from petrochemical flares, J. Geophys. Res.-Atmos., 118, 8716–8728, doi:10.1002/jgrd.50643, 2013.

Pollack, I. B., Lerner, B. M., and Ryerson, T. B.: Evaluation of ultraviolet light-emitting diodes for detection of atmospheric NO_2 by photolysis – chemiluminescence, J. Atmos. Chem., 65, 111–125, doi:10.1007/s10874-011-9184-3, 2010.

Rasmussen, R. A.: What do the hydrocarbons from trees contribute to air pollution?, J. Air Pollut. Contr. Assoc., 22, 537–543, 1972.

Rivera-Rios, J. C., Nguyen, T. B., Crounse, J. D., Jud, W., St. Clair, J. M., Mikoviny, T., Gilman, J. B., Lerner, B. M., Kaiser, J. B., de Gouw, J., Wisthaler, A., Hansel, A., Wennberg, P. O., Seinfeld, J. H., and Keutsch, F. N.: Conversion of hydroperoxides to carbonyls in field and laboratory instrumentation: observational bias in diagnosing pristine versus anthropogenically-controlled atmospheric chemistry, Geophys. Res. Lett., 41, 8645–8651, doi:10.1002/2014GL061919, 2014.

Rohrer, F., Lu, K. D., Hofzumahaus, A., Bohn, B., Brauers, T., Chang, C. C., Fuchs, H., Haseler, R., Holland, F., Hu, M., Kita, K., Kondo, Y., Li, X., Lou, S. R., Oebel, A., Shao, M., Zeng, L. M., Zhu, T., Zhang, Y. H., and Wahner, A.: Maximum efficiency in the hydroxyl-radical-based self-cleansing of the troposphere, Nat. Geosci., 7, 559–563, doi:10.1038/ngeo2199, 2014.

Ryerson, T. B., Williams, E. J., and Fehsenfeld, F. C.: An efficient photolysis system for fast-response NO_2 measurements, J. Geophys. Res.-Atmos., 105, 26447–26461, doi:10.1029/2000jd900389, 2000.

Sakulyanontvittaya, T., Duhl, T., Wiedinmyer, C., Helmig, D., Matsunaga, S., Potosnak, M., Milford, J., and Guenther, A.: Monoterpene and sesquiterpene emission estimates for the United States, Environ. Sci. Technol., 42, 1623–1629, doi:10.1021/es702274e, 2008.

Saunders, S. M., Jenkin, M. E., Derwent, R. G., and Pilling, M. J.: Protocol for the development of the Master Chemical Mechanism, MCM v3 (Part A): tropospheric degradation of non-aromatic volatile organic compounds, Atmos. Chem. Phys., 3, 161–180, doi:10.5194/acp-3-161-2003, 2003.

Schauer, J. J., Kleeman, M. J., Cass, G. R., and Simoneit, B. R. T.: Measurement of emissions from air pollution sources. 2. C-1 through C-30 organic compounds from medium duty diesel trucks, Environ. Sci. Technol., 33, 1578–1587, doi:10.1021/es980081n, 1999.

Stammes, P., Sneep, M., De Haan, J. F., Veefkind, J. P., Wang, P., and Levelt, P. F.: Effective cloud fractions from the Ozone Monitoring Instrument: Theoretical framework and validation, J. Geophys. Res.-Atmos., 113, D16S38, doi:10.1029/2007jd008820, 2008.

Stavrakou, T., Müller, J.-F., De Smedt, I., Van Roozendael, M., Kanakidou, M., Vrekoussis, M., Wittrock, F., Richter, A., and Burrows, J. P.: The continental source of glyoxal estimated by the synergistic use of spaceborne measurements and inverse modelling, Atmos. Chem. Phys., 9, 8431–8446, doi:10.5194/acp-9-8431-2009, 2009.

Tawfik, A. B., Stöckli, R., Goldstein, A., Pressley, S., and Steiner, A. L.: Quantifying the contribution of environmental factors to isoprene flux interannual variability, Atmos. Environ., 54, 216–224, doi:10.1016/j.atmosenv.2012.02.018, 2012.

Volkamer, R., Baidar, S., Campos, T. L., Coburn, S., DiGangi, J. P., Dix, B., Eloranta, E. W., Koenig, T. K., Morley, B., Ortega, I., Pierce, B. R., Reeves, M., Sinreich, R., Wang, S., Zondlo, M. A., and Romashkin, P. A.: Aircraft measurements of BrO, IO, glyoxal, NO_2, H2O, O_2–O_2 and aerosol extinction profiles in the tropics: comparison with aircraft-/ship-based in situ and lidar measurements, Atmos. Meas. Tech., 8, 2121–2148, doi:10.5194/amt-8-2121-2015, 2015.

Vrekoussis, M., Wittrock, F., Richter, A., and Burrows, J. P.: GOME-2 observations of oxygenated VOCs: what can we learn from the ratio glyoxal to formaldehyde on a global scale?, Atmos. Chem. Phys., 10, 10145–10160, doi:10.5194/acp-10-10145-2010, 2010.

Washenfelder, R. A., Wagner, N. L., Dube, W. P., and Brown, S. S.: Measurement of Atmospheric Ozone by Cavity Ring-down Spectroscopy, Environ. Sci. Technol., 45, 2938–2944, doi:10.1021/es103340u, 2011.

Wiedinmyer, C., Greenberg, J., Guenther, A., Hopkins, B., Baker, K., Geron, C., Palmer, P. I., Long, B. P., Turner, J. R., Petron, G., Harley, P., Pierce, T. E., Lamb, B., Westberg, H., Baugh, W., Koerber, M., and Janssen, M.: Ozarks Isoprene Experiment (OZIE): Measurements and modeling of the "isoprene volcano", J. Geophys. Res.-Atmos., 110, D18307, doi:10.1029/2005jd005800, 2005.

Wolfe, G. M. and Thornton, J. A.: The Chemistry of Atmosphere-Forest Exchange (CAFE) Model – Part 1: Model description and characterization, Atmos. Chem. Phys., 11, 77–101, doi:10.5194/acp-11-77-2011, 2011.

Zhou, S., Gonzalez, L., Leithead, A., Finewax, Z., Thalman, R., Vlasenko, A., Vagle, S., Miller, L.A., Li, S.-M., Bureekul, S., Furutani, H., Uematsu, M., Volkamer, R., and Abbatt, J.: Formation of gas-phase carbonyls from heterogeneous oxidation of polyunsaturated fatty acids at the air–water interface and of the sea surface microlayer, Atmos. Chem. Phys., 14, 1371–1384, doi:10.5194/acp-14-1371-2014, 2014.